

# TRÓJWYMIAROWA ANALIZA NUMERYCZNA ELEKTROFILTRU TYPU PRZEWÓD-CYLINDER DO WYŁĄPYWANIA BARDZO DROBNYCH CZĄSTEK ZE SPALIN SILNIKA DIESLA

**Niloofar Farnoosh, G.S. Peter Castle, Kazimierz Adamiak**

University of Western Ontario, Department of Electrical and Comp. Eng.

**Abstract.** A precipitator section is modeled numerically in 3D to determine the collection efficiency for diesel exhaust particulates. It consists of a circular tube and a wire electrode mounted at the center of the tube, supplied with a negative high dc voltage, while the tube is electrically grounded. The analytical solutions of Poisson and current continuity equations are implemented to obtain the ionic space charge density and electric potential distributions in the channel. Commercial CFD FLUENT software is used to solve the turbulent flow mode. Effects of some electrical characteristics of diesel exhaust particulates on collection efficiency are assessed.

**Keywords:** electrostatic precipitators, electrohydrodynamics, corona discharge, particle trajectories, collection efficiency.

## 3D Numerical Study of Wire-Cylinder Precipitator for Collecting Ultrafine Particles from Diesel Exhaust

**Streszczenie.** Jedna sekcja elektrofiltru została zamodelowana numerycznie w celu wyznaczenia sprawności wylapywania cząstek ze spalin silnika Diesla. Elektrofiltr składa się z uziemionej cylindrycznej rury i cienkiej elektrody zasilanej wysokim napięciem ujemnym. Do obliczeń wykorzystano analityczne rozwiązanie równania Poissona i równania ciągłości ładunku oraz komercyjny software FLUENT do obliczeń przepływu gazu. Cząstki były ładowane w wyniku łącznych mechanizmów polowych i dyfuzyjnych. Zbadany został efekt niektórych parametrów procesu na sprawność filtrowania.

**Słowa kluczowe:** elektrofiltry, elektrohydrodynamika, wyładowanie koronowe, trajektorie cząstek, sprawność osadzania.

## Introduction

Diesel Exhaust Particulate (DEP) is one of many causes of air pollution in urban areas. In recent years, special environmental concerns have been directed towards controlling the emission of ultrafine particles. This is also related to different strategies used by engine designers to increase engine efficiency.

Optimization of the engine combustion process using alternative fuels, or special fuel additives, and installing after-treatment systems, such as catalytic converters, wet scrubbers, cyclones, bag filters, Diesel Particulate Filters (DPFs) and Electrostatic Precipitators (ESPs), are among conventional methods attempted to reduce particulate emissions. Despite the very good performance of DPFs, they still suffer from high pressure drop, high energy consumption and maintenance costs, low durability and insufficient collection efficiency for nanoparticles. On the other hand, ESPs are more reliable particulate control devices due to their high collection efficiency, lower pressure drop, lower energy consumption and capability to operate over a wide range of gas temperature [1]-[3].

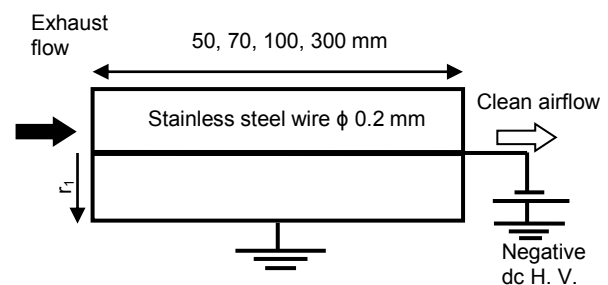
Due to the low electrical resistivity of diesel particulates, they lose their charge as soon as they arrive at the collecting plates, and can easily re-enter the channel, resulting in a substantial decrease in particle removal efficiency. To overcome this problem, several authors have worked on the electrostatic agglomeration of aerosols emitted by diesel engines [4]-[6] by moving their distribution towards large diameters (several micrometers at least). In [7], A. Mizuno et al. employed electrostatic flocking electrodes as the collecting plates in an ESP to improve the collection efficiency of fine particles by increasing the surface area of the collecting electrodes. The same authors also suggested an ESP-DPF combined system to obtain higher collection efficiency for diesel particulates, where the number density of particles measured in downstream of the combined system was 98 % less compared with that of DPF alone [8]. In addition, they confirmed that increase in the pressure drop of the DPF is slower due to agglomeration.

Wire-tube electrostatic precipitators, where a thin wire is placed in center of the tube and charged with high voltage are proposed by some authors to capture ultra fine particles and diesel particulates [8]-[11]. Saiyasitpanich et al. performed experiments [2], [3] to examine a tubular single-stage wet electrostatic precipitator (wESP) performance in removal of diesel particulate matter. Their measured collection efficiencies were significantly higher than the predicted values based on the well-known Deutsch equation [12].

In this paper, a 3D numerical simulation is carried out for modeling a wire-tube ESP for collecting diesel particulates. The corona-induced secondary flow in an ESP with eccentric wire-cylinder geometry is discussed. Particles charging and deposition patterns are obtained and the collection efficiency of the ESP is predicted. The influence of the applied voltage to the corona electrode, the gas inlet velocity and channel length on the precipitation performance is also investigated.

## 1. Model description

The wire-cylinder electrostatic precipitator utilized by H. Hayashi et al. [8] to collect exhaust gas emissions from a diesel engine generator (Fuji Heavy Industries Ltd., SGD3000S-III, max power output: 3 kW), as shown in Fig. 1, is simulated. The discharge electrode was a stainless steel wire with the diameter of 0.2 mm energized with a negative high dc voltage to generate corona discharge. A stainless steel tube with the diameter of 36 mm and length of 50-300 mm was used as a collection electrode. The exhaust gas with dust mass concentration of 20 mg/m<sup>3</sup> and initial velocity of 0.6-1.5 m/s was passed through the precipitator. Diesel aerosols are in the range of 5-550 nm with density of 998.9 kg/m<sup>3</sup>.



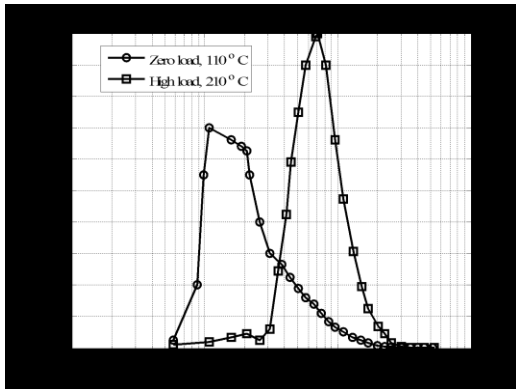
Rys. 1. Schemat elektrofiltru

Fig. 1. Schematic diagram of a wire-cylinder ESP

Two number concentrations of diesel particulates were assumed at the inlet for engine working in low load (0 W, 110°C) and high load (2.6 kW, 210°C), as shown in Fig. 2. Each particle size was injected from 248 points at the inlet resulting in a total number of 7440 and 6696 particle streams in the ESP channel for engine at zero load and high load conditions, respectively.

## 2. Computational procedure

The exact analytical solution for solving the Poisson and current continuity equations for wire-cylinder geometry was utilized to obtain the electric potential, electric field, and ion charge density distributions in the precipitation channel for



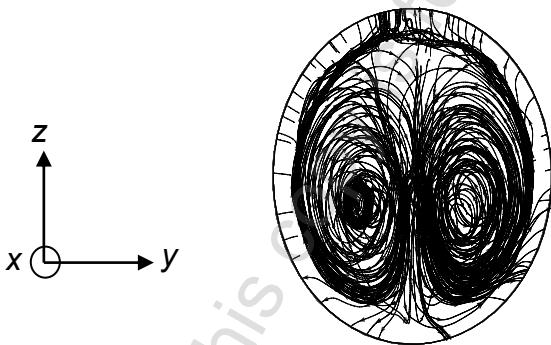
Rys. 2. Zależność koncentracji ilościowej od średnicy cząstek na wejściu  
Fig. 2. Number concentration versus particles diameter at inlet

different applied voltages [13]. It was assumed that the ionic charge distribution in the channel would not be disturbed by the airflow and only the strong effect of electrostatic forces due to the presence of ionic space charge in electric fields on the airflow patterns was considered. The airflow equations were solved inside FLUENT using the Finite Volume Method (FVM) and the turbulence effect was included by using the  $k-\epsilon$  model. The Lagrangian random walk approach was used to determine particle motion, as affected by EHD flows and gas turbulence. This part was performed with the aid of DPM module in FLUENT considering submicron particle charging equations. The detailed description of the methodology and procedures can be found in [14].

## 3. Results and Discussion

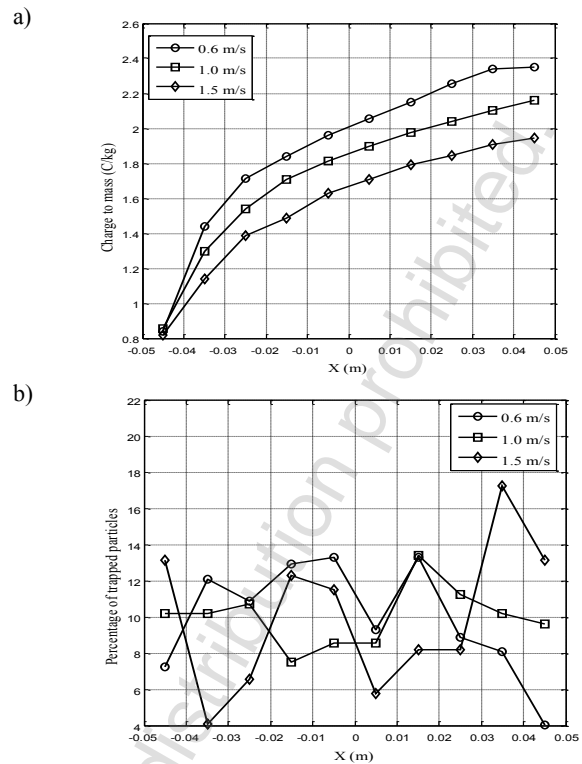
### 3.1. EHD Flow Pattern

In a concentric configuration of electrodes, the secondary flow does not exist due to symmetry of the geometry and static conditions in the channel, where the electric body force is balanced by the pressure force along the radial direction, as it was also proven in [15]. Assuming 1% electrode eccentricity in the  $z > 0$  direction, a corona-induced jet is developed along the eccentricity direction with two spiral vortices on either sides of the jet, where the vortex on the right rotates counter clockwise, and the vortex on the left rotates clockwise, as shown in Fig. 3. These vortices occupy almost the whole area of the ESP cross section.



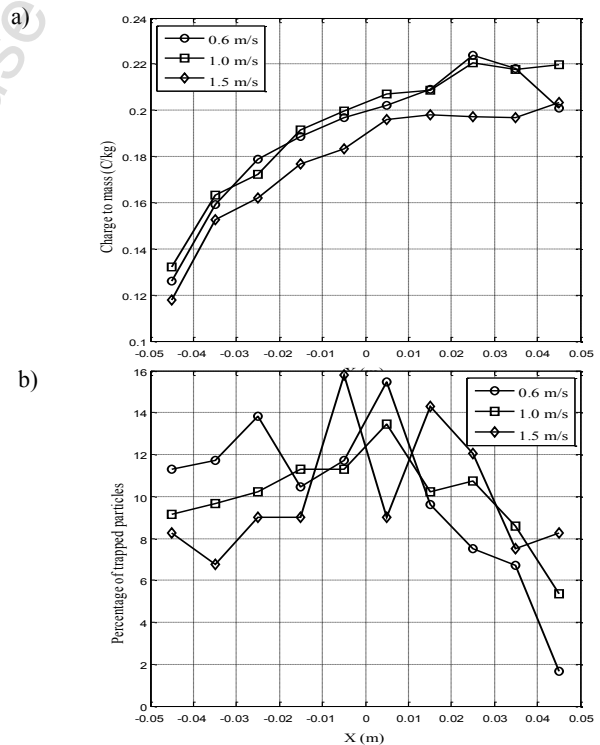
Rys. 3. Linie strumienia wtórnego przepływu elektrohydrodynamicznego dla ekscentrycznego położenia elektrody wyladowczej

Fig. 3. EHD secondary flow streamlines for eccentric configuration of the corona discharge electrode



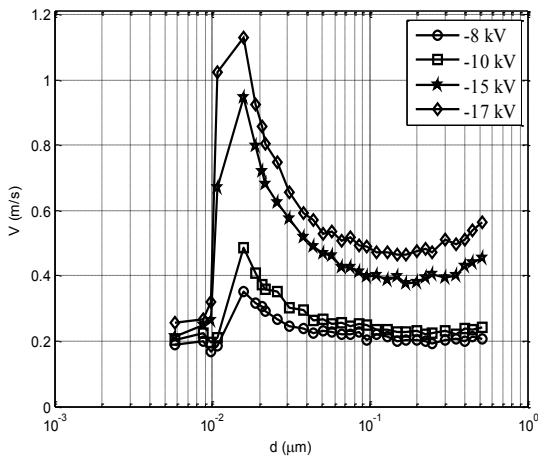
Rys. 4. Stosunek ładunku do masy (a) i procent wylapanych cząstek wzdłuż kanału elektrofiltru (b) dla cząstek o średnicy 100 nm i trzech prędkości gazu (silnik w stanie jałowym, przyłożone napięcie -10 kV, długość kanału 100 mm, temperatura 110° C)

Fig. 4. Charge-to-mass ratio (a) and percentage of trapped particle along the ESP channel (b) for 100 nm particles and for three inlet velocities (engine at zero load condition, applied voltage is -10 kV, channel length is 100 mm, and temperature is 110° C)



Rys. 5. Stosunek ładunku do masy (a) i procent wylapanych cząstek wzdłuż kanału elektrofiltru (b) dla cząstek o średnicy 500 nm i trzech prędkości gazu (silnik w stanie jałowym, przyłożone napięcie -10 kV, długość kanału 100 mm, temperatura 110° C)

Fig. 5. Charge-to-mass ratio (a) and percentage of trapped particle along the ESP channel (b) for 500 nm particles and for three inlet velocities (engine at zero load condition, applied voltage is -10 kV, channel length is 100 mm, and temperature is 110° C)



Rys. 6. Prędkość migracji cząstek dla różnych wartości napięcia (długość kanału 100 mm, prędkości gazu 0.6 m/s, 1 m/s i 1.5 m/s)

Fig. 6. Particle migration velocity for different applied voltages (channel length of 100 mm and inlet velocities of 0.6 m/s, 1 m/s and 1.5 m/s)

### 3.2. Particle Charging and Deposition

Particle charge-to-mass ratio and deposition rate along the ESP channel length for 100 nm and 500 nm particles are shown in Figs. 4 and 5, respectively, assuming different inlet velocities of 0.6 m/s, 1.0 m/s and 1.5 m/s, zero engine load and -10 kV excitation voltage to the corona wire. Fig. 4a shows that by increasing the inlet velocity particles travel faster in the ESP channel and the charge-to-mass ratio decreases. The charge-to-mass ratio of particles increases as the particles traverse the channel. However, larger particles obtain the saturated charge quicker and the velocity effect on charge-to-mass ratio becomes negligible (Fig. 5a). Similar graphs were obtained for engine at high load condition.

In the presented simulation model, particles smaller than 20 nm obtain no charge or at most one electron charge, as they traverse the whole length of the ESP channel, and their trajectories are only affected by airflow drag forces, thus, practically these particles could not be trapped. Therefore, the numerical results in this paper are only valid for particles larger than 20 nm.

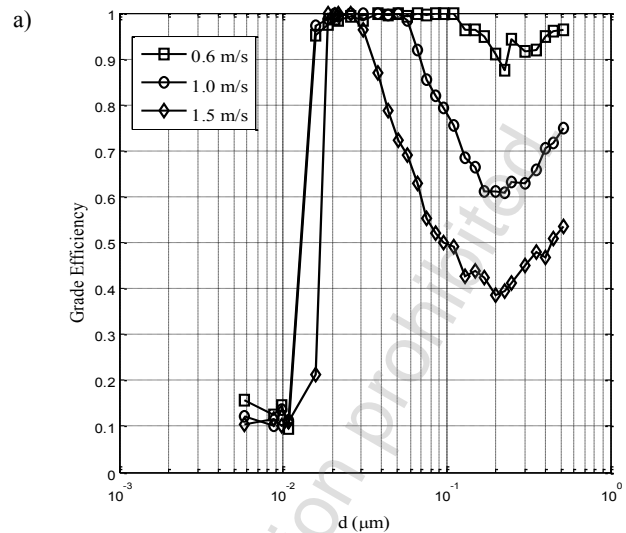
### 3.3. Particle Migration Velocity

Fig. 6 shows the particle migration velocity under different voltages applied to the corona wire assuming three different inlet velocities of 0.6, 1.0 and 1.5 m/s and engine at zero load condition. The particle migration velocity increases by increasing the applied voltage and it has a minimum around 200-300 nm particle diameter, which is theoretically explained in [16]. Similar graphs were obtained for the engine at the high load condition.

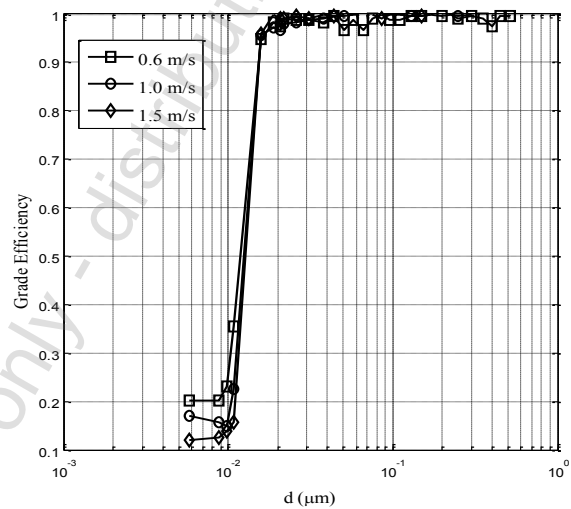
### 3.4. Grade Efficiency

Figs. 7a and 7b show the corresponding grade efficiencies of different particle sizes for applied voltages of -10 kV and -17 kV, and inlet velocities of 0.6, 1.0 and 1.5 m/s, assuming engine at zero load condition. For excitation voltages of -10 kV (Fig. 7a), the grade efficiency has a minimum value at around 200-300 nm particle diameter and the grade efficiency decreases by increasing the inlet velocity from 0.6 m/s to 1.5 m/s. This can be explained by looking at the particle migration velocities, shown in Fig. 6, and the relation between the particle migration velocity and grade collection efficiency in the Deutsch equation [12]. However, for -17 kV excitation voltage the grade efficiency for all particle sizes is more than 95% as shown in Fig. 7b.

Figs. 8a and 8b show the particle residence time and grade efficiencies versus exhaust particle diameter for channel length in the range of 50-300 mm, engine at low load condition and -10 kV applied voltage to the corona wire. It is clear that the residence time and grade efficiency of particles increases by increasing the



b)



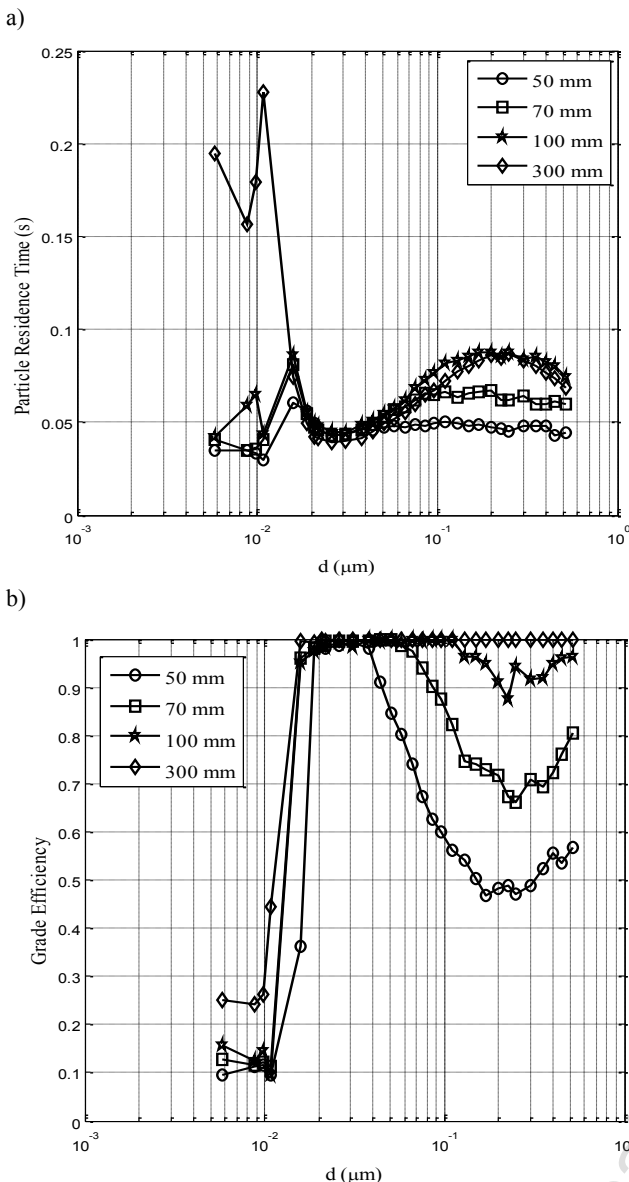
Rys. 7. Sprawność osadzania dla różnych wielkości cząstek i różnych prędkości gazu (długość kanału 100 mm, silnik na biegu jałowym, napięcie zasilania -10 kV (a) i -17 kV (b))

Fig. 7. Grade efficiency of ESP for three inlet velocities at inlet (channel length of 100 mm, engine at zero load condition and applied voltages of -10 kV (a) and -17 kV (b))

channel length and for 300 mm almost all particles are trapped in the ESP channel. The minimum grade efficiency and maximum particle residence time around 200-300 nm particle diameter can be observed for different channel length as well. Similar graphs were obtained for the engine at the high load condition.

## 4. Conclusions

A one-stage laboratory scale single wire-cylinder ESP for collecting submicron diesel particulates was simulated. It was shown that the EHD secondary flow is only generated in the channel when the corona wire is slightly off-center in the cylindrical channel. For different particle sizes, particle charge-to-mass ratio and deposition rate along the ESP channel were compared for different inlet velocities. It was shown that by increasing the gas residence time, i.e. decreasing the inlet velocity, the particle charge-to-mass ratio increases and the particle removal efficiency increases. Particle migration velocities were obtained for different applied voltages. Total mass collection efficiency for different channel lengths and the grade efficiencies of all particle sizes were also obtained. It was shown that the collection efficiency graphs versus diesel particle diameter have a minimum around 200-300 nm for lower excitation voltages. However, for higher excitation voltage and lower gas velocities at inlet, the collection efficiency for all particle sizes is above 95%.



Rys. 8. Czas (a) i sprawność osadzania (b) dla różnych wielkości cząstek i czterech różnych długości kanału (napięcie zasilania -10 kV, prędkość gazu 0.6 m/s, silnik lekko obciążony)

Fig. 8. Particle residence time (a) and grade efficiency (b) versus exhaust particle diameter for four different length of the ESP channel (applied voltage is -10 kV, inlet velocity is 0.6 m/s and engine is at low load condition)

## References

- [1] Desantes J.M., Margot X., Gil A., Fuentes E.: *Computational study on the deposition of ultrafine particles from Diesel exhaust aerosol*. J. Aerosol Sci., vol. 37/2006, pp. 1750 – 1769.
- [2] Saiyasitpanich P., Keener T.C., Lu M., Khang S.-J., Evans D.E.: *Collection of ultrafine diesel particulate matter (DPM) in cylindrical single-stage wet electrostatic precipitators*. Environ. Sci. Technol., vol. 40/2006, pp. 7890-7895.
- [3] Saiyasitpanich P., Keener T.C., Khang S.-J., Lu M.: *Removal of diesel particulate matter (DPM) in a tubular wet electrostatic precipitator*. J. Electrostat., vol. 65/2007, pp. 618-624.
- [4] Wadenpohl C., Löffler F.: *Electrostatic agglomeration and centrifugal separation of diesel soot particles*, Chem. Eng. Process., vol. 33/1994, pp. 371–377.
- [5] Boichot R., Bernis A., E. Gonze, *Treatment of diesel particles using an electrostatic agglomerator under negative DC corona: a modeling and experimental study*, IEEE Trans. Plasma Sci., vol. 35/2007, pp. 675–692.
- [6] Boichot R., Bernis A., Gonze E., *Agglomeration of diesel particles by an electrostatic agglomerator under positive DC voltage: Experimental study*, J. Electrostat., vol. 66/2008, pp. 235–245.

- [7] Sung B.-J., Aly A., Lee S.-H., Takashima K., Kastura S., Mizuno A.: *Fine-particle collection using an electrostatic precipitator equipped with an electrostatic flocking filter as the collecting electrode*, Plasma Processes Polym., vol. 3/2006, pp. 661–667.
- [8] Hayashi H., Takasaki Y., Kawahara K., Takenaka T., Takashima K., Mizuno A.: *Electrostatic charging and precipitation of diesel soot*, IEEE Trans. Ind. Appl., vol. 47/2011, pp. 331-335.
- [9] Marquard A., Kasper M., Meyer J., Kasper G.: *Nanoparticle charging efficiencies and related charging conditions in a wire-tube ESP at DC energization*, J. Electrostat., vol. 63/2005, pp. 693-698.
- [10] Tilmatine A., Gouri R., Miloua F., Kadous N., Medles K., Dascalescu L.: *Optimization of the intermittent operation of a wire-cylinder electrostatic precipitator*, J. Phys.: Conf. Ser., vol. 142/2008, pp. 12-19.
- [11] Kuroki T., Ishidate M., Okubo M., Yamamoto T.: *Charge-to-mass ratio and dendrite structure of diesel particulate matter charged by corona discharge*, CARBON, vol. 48/2010, pp. 184–190.
- [12] Deutsch W.: *Bewegung und ladung der elektrizitatstrager im zylinderkondensator*, Annal. Phys., vol. 68/1922, pp. 335-344.
- [13] Janischewskij W., Gela G.: *Finite element solution for electric fields of coronating dc transmission lines*, IEEE Trans. Power Appar. Syst., vol. 98/1979, pp. 1000-1012.
- [14] Farnoosh N., Adamiak K., G.S.P. Castle G.S.P.: *3-D numerical analysis of EHD turbulent flow and mono-disperse charged particle transport and collection in a wire-plate ESP*, J. Electrostat., vol. 68/2010, pp. 513-522.
- [15] Baghaei Lakeh R., Molki M.: *Patterns of airflow in circular tubes caused by a corona jet with concentric and eccentric wire electrodes*, J. Fluids Eng., vol. 132/2010, DOI: 10.1115/1.4002008.
- [16] Mizuno A.: *Electrostatic precipitation*, IEEE Trans. Dielectr. Electr. Insul., vol. 7/2000, pp. 615-624.

**Dr inż. Niloofar Farnoosh**  
e-mail: nf.farnoosh@gmail.com

**Niloofar Farnoosh** was born in Iran in 1981. She received the M.Sc. degree in electrical engineering from Amirkabir University of Technology, Tehran, Iran, in 2007, and the PhD degree from The University of Western Ontario, London, ON, Canada in 2011. Her research interests include computational electromagnetics, particle charging and deposition in electrostatic precipitators, electrohydrodynamics and applied electrostatics.



**Prof. dr inż. G.S.Peter Castle**  
e-mail: pcastle@eng.uwo.ca

**G.S.Peter Castle** is a Professor Emeritus and Adjunct Research Professor in Electrical and Computer Engineering, University of Western Ontario, London, Ontario, Canada. He earned his B.E.Sc. and Ph.D. in Electrical Engineering from the University of Western Ontario and M.Sc. from Imperial College in 1963. He has been active in research in the field of applied electrostatics for over 44 years having published extensively in the areas of electrostatic precipitation, electrostatic painting and coating, electrophotography and electrostatic separation.



**Prof. dr hab. inż. Kazimierz Adamiak**  
e-mail: kadamiak@eng.uwo.ca

**Kazimierz Adamiak** received the M.Sc. and Ph.D. degrees in electrical engineering from the Szczecin University of Technology, Szczecin, Poland, and the D.Sc. degree (habilitation) from the Gdansk University of Technology, Gdansk, Poland. Currently, he works as a professor in the Department of Electrical and Computer Engineering, the University of Western Ontario, London, Ontario, Canada. His research interests include applied electrostatics, electrohydrodynamics and computational electromagnetics.

